

The Structure of Phytoplankton Communities in the Eastern Part of the Laptev Sea

I. N. Sukhanova^a, M. V. Flint^{a,*}, E. Ju. Georgieva^b, E. K. Lange^c, M. D. Kravchishina^a, A. B. Demidov^a,
A. A. Nedospasov^a, and A. A. Polukhin^a

^a*Shirshov Institute of Oceanology, Russian Academy of Sciences, Moscow, 117218 Russia*

^b*Kovalevsky Institute of Marine Biological Research, Russian Academy of Sciences, Sevastopol, 299011*

^c*Atlantic Branch, Shirshov Institute of Oceanology, Russian Academy of Sciences, Kaliningrad, 236022 Russia*

*e-mail: m_flint@ocean.ru

Received May 17, 2016; in final form, September 18, 2016

Abstract—Studies have been performed on a transect along 130°30' E from the Lena River delta (71°60' N) to the continental slope and adjacent deepwater area (78°22' N) of the Laptev Sea in September 2015. The structure of phytoplankton communities has distinct latitudinal zoning. The southern part of the shelf (southward of 73°10' N), the most desalinated by riverine discharge, houses a phytoplankton community with a biomass of 175–840 mg/m², domination of freshwater *Aulacoseira* diatoms, and significant contribution of green algae (both in abundance and biomass). The northern border for the distribution range of the southern complex of phytoplankton species lies between the 8 and 18 psu isohalines (~73°10' N). The continental slope and deepwater areas of the Laptev Sea (north of 77°30' N), with a salinity of >27 psu in the upper mixed layer, are populated by the community prevalently composed of *Chaetoceros* and *Rhizosolenia* diatoms, very abundant in the Arctic, and dinoflagellates. The phytoplankton number in this area fall in the range of 430–1100 × 10⁶ cell/m², and the biomass, in the range of 3600 mg/m². A moderate desalinating impact of the Lena River discharge is observed in the outer shelf area between 73°20' and 77°30' N; the salinity in the upper mixed layer is 18–24 psu. The phytoecenosis in this area has a mosaic spatial structure with between-station variation in the shares of different alga groups in the community, cell number of 117–1200 × 10⁶ cells/m², and a biomass of 1600–3600 mg/m². As is shown, local inflow of “fresh” nutrients to the euphotic layer in the fall season leads to mass growth of diatoms.

DOI: 10.1134/S0001437017010209

INTRODUCTION

The Laptev Sea is an epicontinental Arctic waterbody of high interest to researchers. This is determined by its central position in the system of Siberian seas and a great effect of the riverine discharge, first and foremost, the discharge of the Lena River, the largest Siberian river, on the regime of this sea and the overall ecosystem. Research in the Laptev Sea intensified in the 1990s under various international projects. The Russian–German program The Laptev Sea System (which commenced in the early 1990s and continued for over 15 years) [7] has considerably contributed to this area. This program in its marine part was mainly focused on the ice regime, hydrology, sedimentation processes, geochemistry, geology, and riverine discharge, as well as the climate and paleoclimate. The biological aspect of oceanological research, to say nothing of ecosystem studies, was rather modest in volume; thus, the key links between environment and biota, which determine the structure and production of the Laptev Sea ecosystem, and the roles of leading components of the biota in the matter flows still remain understudied.

The studies of the phytoplankton of this sea and the factors determining the structural and functional

parameters of this key ecosystem component are very sparse. See [1, 2, 4, 6, 8, 15, 16, 18, 20, 22, 23] for data on the composition and quantitative distribution of plankton algae.

A number of papers [2, 5] list the observed phytoplankton species and the dominant species do not analyze of the structure of the phytoecenosis. Data on the phytoplankton composition and quantitative characteristics on the Lena River delta and Bukhor-Khaya Bay in summer (end of July–beginning of August) are available [2, 18]. Seasonal changes in the phytoplankton composition and quantitative characteristics in the Lena River delta and adjacent Laptev Sea shelf have been characterized by Tuschling [23]. The author himself regards the sampling performed in different years and different seasons, large distances between sampling stations in summer and fall, and the absence of accompanying comprehensive hydrophysical and hydrochemical data as considerable shortcomings of the work. She did not consider the early fall season of succession (the first half of September) and the structure of the phytoecenosis in the deepwater Laptev Sea regions. Tuschling's values of the phytoplankton abundance and biomass [23] demonstrate considerable vari-

Table 1. Seasonal changes in the phytoplankton abundance ($N \times 10^3$ cells/L), carbon biomass (B, mgC/m³) and chlorophyll *a* concentration (mgC/m³) in estuarine zone, desalinated surface “lens”, and at station over continental slope of Laptev Sea in transect along 130°30' E (according to Tuschling [23])

Region*	Season	<i>N</i>	B	Chl <i>a</i>
Estuarine zone	Spring (May–June)	100–500	1–65	0.04–0.34
	Summer (early August)	250–400	25–80	2.2–2.7
	Fall (October)	15.0	5.0	No data
Desalinated surface “lens”	Summer (early August)	100–2500	10.0–225.0	0.24–0.64
	Fall (October)	8.0	1.0	No data
Continental slope	Summer (early August)	600	125	0.84

* Regions are named according to [23].

ation of the quantitative characteristics in different periods of seasonal succession and no less pronounced interannual variation in seasonal data (Table 1). Two other papers [16, 22] report data on characteristics of the phytocenosis in the same regions and time as in our studies. A high abundance of the euryhaline symbiotic infusoria *Mesodinium rubrum* was recorded in the Lena River delta and directly adjacent inner shelf, which explained the comparatively high level of integral primary production [22]. Sorokin and Sorokin [22] also determined the boundary for mass distribution of freshwater phytoplankton over the shelf, which coincided with the 15 psu isohaline. The determined northern boundary of the plume desalinated by riverine discharge lay between 75° and 76° N [16]. The change in salinity in the peripheral frontal zone of the plume was 10 psu along ~50 km, and the authors associated the boundary for the region with the dominance of freshwater phytoplankton with the 13 psu surface isohaline. A mass accumulation of *Chaetoceros socialis* (8.5×10^6 cells/L) formed by vegetative cells and resting spores was discovered at the northernmost station of the transect in the continental shelf area. The resting spores accounted for ~30% of the total population. However, these papers [16, 22] lack any analysis of the latitudinal changes in species composition of phytocenosis as well as data on phytoplankton in the deep-water part of the Laptev Sea.

The goal of this work was to analyze the composition and distribution of phytoplankton in different latitudinal zones in the eastern part of the Laptev Sea from the Lena River delta to its deep abyssal; to quantitatively characterize the latitudinal zoning of phytocenosis in terms of abundance, biomass, and chlorophyll *a* concentration; to assess the ranges of dominance and the boundaries to which the freshwater phytoplankton complex spread northward into the shelf area and to which the marine species spread over

the shelf; and to compare the quantitative characteristics of the phytocenosis obtained in different years for the early fall period of seasonal succession.

STUDY AREA, MATERIALS, AND METHODS

The work was performed in the eastern part of the Laptev Sea during September 8–14, 2015. The stations were located along a meridional transect at 130°30' E between 72°00' and 78°45' N. Only the southernmost station, 5216, in Buor-Khaya Bay was shifted by half a degree westward into the region intensively influenced by freshwater Lena River discharge coming in through the Bykov Channel (Fig. 1).

Phytoplankton was sampled with an SBE 911 probe equipped with a Rosette SBE 32 with 12 5-L Niskin bottles. The depths for phytoplankton sampling were selected based on the data of preliminary temperature, salinity, and fluorescence probing. Samples were collected from three to five depths: the upper mixed layer (one to two samples), the layer of the density jump and the fluorescence maximum (one to two samples), and the layer under the pycnocline (one to two samples). To analyze phytoplankton, 2 L of water were sampled from each Niskin bottle. The samples for assaying the chlorophyll *a* concentration and concentrations of nutrients were also taken from the same bottles.

Phytoplankton was concentrated by gentle reverse filtration technique of 2-L samples through Dacron filters (pore size, 1 μm) [9]. The final volume of a concentrated sample was 40–90 mL. All samples were processed in a living state either immediately after sampling or over 1–2 days. Until assayed, the samples were stored in a refrigerator at a temperature of 2–3°C. The samples were examined in Nageotte chambers (volume, 0.085 mL) at a magnification of ×400 and Nauman's (volume, 1 mL) chambers at a magnification of ×200. Dead diatom cells were also counted to

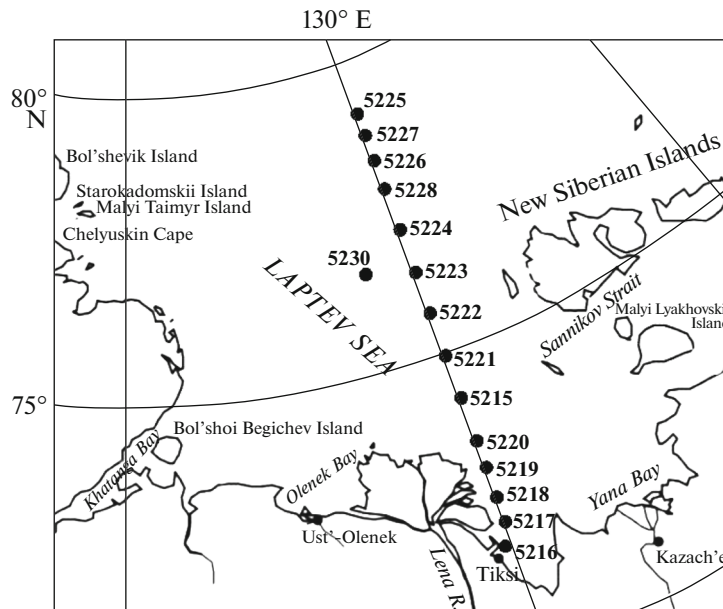


Fig. 1. Transect and stations location.

assess the state of populations during the study period. Chlorophyll and particulate matter were assayed as described in [5, 17, 12]. The carbon content in cells was calculated using the corresponding coefficients for different taxa and size groups [19, 24].

RESULTS

Hydrophysical and Hydrochemical Characterization of the Study Area

The Laptev Sea is the shallowest of the Eurasian Arctic seas. The 60-m isobathic line runs 450–550 km from the coast [1]. In general, a characteristic of this sea is the lowest salinity of the upper mixed layer as compared with other Arctic seas [14].

The structure of the Lena River delta has no analogs among the rivers of the Russian Arctic. The delta consists of several large channel sand numerous traverse small arms running on a peninsula extending into the sea. The deltas of two large branches—the Bykov Channel (length 106 km) and Trofimov Channel (length, 148 km)—are on the eastern part of the peninsula; the discharge of these branches into the sea are traceable as independent isolated plumes.

The average volume of the Lena River discharge is 542 km³/year. The spring high water takes place in June. The June and July discharge into the sea account for 36.4 and 20.2% of the annual Lena River discharge, respectively; the September (our study period) discharge amounts to 11.9% [6]. During the summer low water period (our study period), 25% of the total discharge (25.6 km³) passes through the

Bykov Channel, and up to 65% (66.8 km³), through the Trofimov Channel.

Figure 2 shows the distribution of salinity and temperature along the transect at 130°30' E during our study. The inner shelf region adjacent to the Lena River delta (stations 5216–5219) had a considerably desalinated 2–4-m upper mixed layer (salinity, 2.5–8 psu), temperature of 7.1–8.3°C, a sharp pycnocline with a thickness of 2–3 m, and a sharp vertical salinity gradient of 3–5 psu/m. The Secchi depth in this region did not exceed 3 m, and the photosynthetic layer was no thicker than 10 m. The water column there had a low transparency due to the high concentration of suspended matter entering with the riverine discharge (5–16 mg/L in the surface layer).

Considerably desalinated surface waters were traced to 73° N (station 5219). Salinity in the upper layer sharply increased by 10 psu to ~18 psu, while temperature dropped by 2°C (to 5.1°C), and the layer of the density jump descended to a depth of 10 m at 73°20' N (station 5220) 35 km to the north. The concentration of suspended matter in the surface layer decreased to 1.5 mg/L.

Station 5215-2 deserves special attention. The pycnocline at this site locally rises to the surface, thereby decreasing the depth of the upper quasi-homogenous layer, increasing salinity in this layer to ~22 psu and decreasing temperature to 3.4°C (Fig. 2). The layer of the density jump in this region extended vertically (from 4 to 15 m), displayed lower vertical salinity and temperature gradients compared with more southern regions, and resided within the photosynthetic layer.

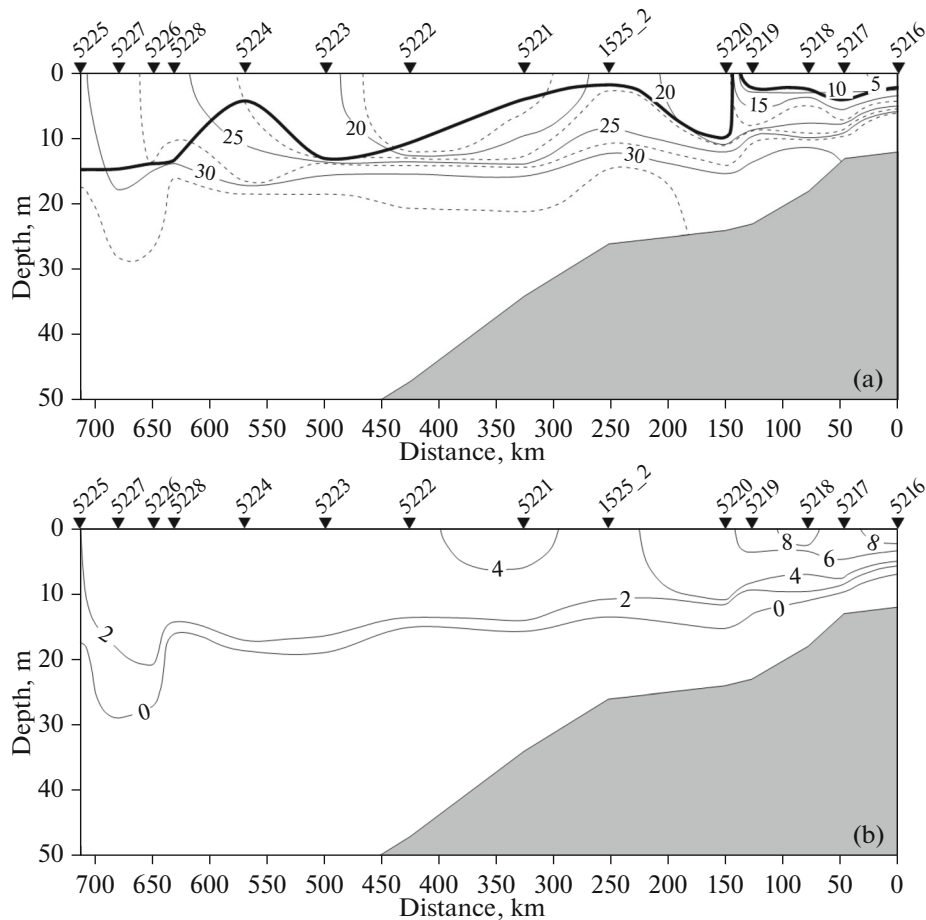


Fig. 2. Distributions of (a) salinity (thick line—upper boundary of pycnocline) and (b) temperature along transect at 130°30' E.

The desalinating effect of riverine discharge occurred again seaward of station 5215-2: at stations 5221–5223 in the upper 10–12 m and at station 5224 in the upper 4 m of the water column, decreasing salinity to 15.9–21.6 psu. The temperature at station 5221 rose to 4.3°C and gradually decreased to 3.7°C to the north, at station 5224. The concentration of suspended matter in the overall water column except for the bottom layer did not exceed 1 mg/L.

The northern boundary of the outer shelf region desalinated by riverine discharge ran between station 5224 (77° N) and slope station 5228 (77°39' N; depth, 90 m). The salinity beyond this region increased from 22 to 27 psu and the temperature decreased to 3°C (Fig. 2). The Arctic water at stations 5225–5227 (above depths of >1000 m) showed a salinity of 27–30 psu, temperature of 2–3°C, and weak density gradients in the layer of the density jump, the upper boundary of which was at a depth of 13–16 m. The concentration of suspended matter in this region was below 0.5 mg/L.

The concentration of nutrients, except for silica, was universally low. The highest SiO₂ concentrations, reaching 58.5–66.6 μM, were recorded in the most

desalinated region of the inner shelf adjacent to the Lena River delta (stations 5216–5219, Fig. 3). The silica concentration in the upper 10–15 m remained at a level of 20 μM to 77° N and decreased in the upper mixed layer to 10.5 μM farther along the transect to 78° N (station 5228). The SiO₂ concentration in the surface layer at stations 5227 and 5225 (depths of 1980 and 2700 m) was 7.6 and 4.1 μM, respectively (Fig. 3).

The amount of nitrates in the photosynthetic layer along the transect varied in a wide range, from 0.15 (station 5227) to 5.2 μM (station 5215-2) (Fig. 3). The highest concentrations, 2.6–4.2 μM, were observed at southern stations of the transect in the region most exposed to the Lena River discharge. The nitrate concentration decreased north of this region to 0.15–2.3 μM, except for station 5215-2, where subsurface water layer was locally enriched for nutrients (Fig. 3). The NO₃ concentration in the surface 10-m layer there reached the maximum value for the overall transect, 5.2 μM.

The concentration of nitrites at all stations of the transect did not exceed 0.9 μM, and the ammonia content varied from 0.5 to 1.4 μM. The content of

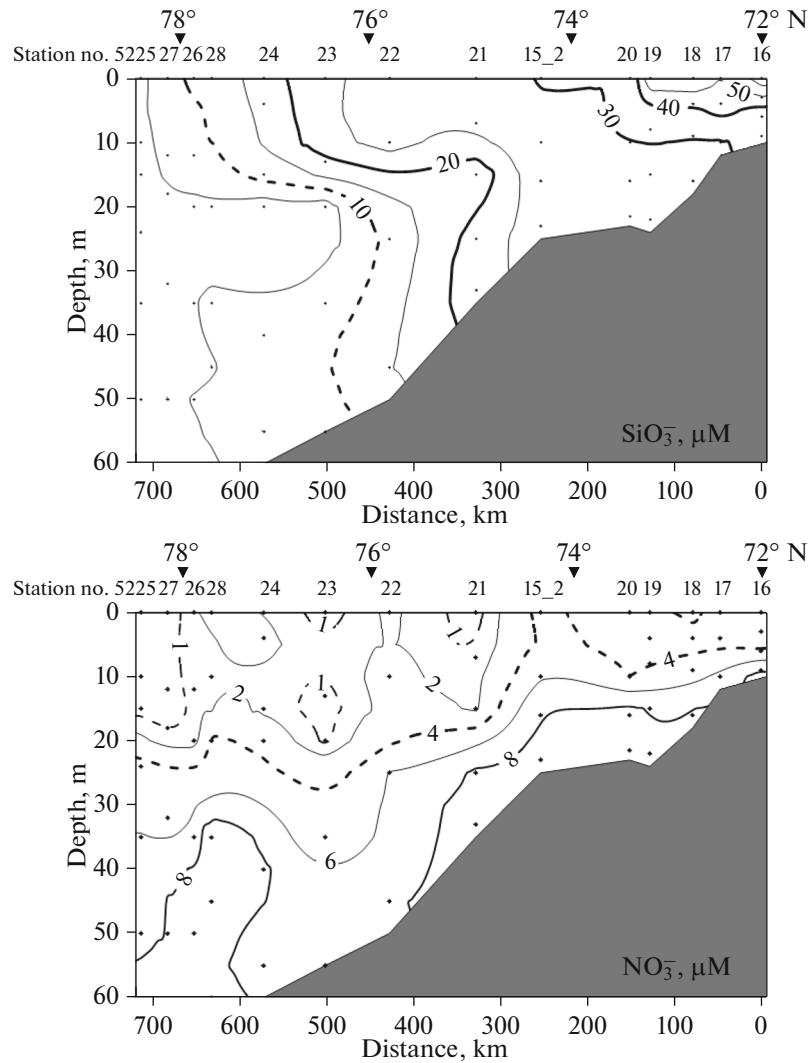


Fig. 3. Distributions of dissolved silica (SiO_3) and nitrates (NO_3) along transect at $130^\circ 30' \text{ E}$.

phosphates varied in the range of $0.09\text{--}0.16 \mu\text{M}$, being at a level limiting phytoplankton growth.

Species Composition of Phytoplankton

In total, 136 freshwater and marine algal species were identified in the examined region, including 60 diatoms, 36 dinoflagellates, and 21 green algae. Few species of the following taxonomic groups were found Chrysophyceae (five species), Dictyochophyceae (two species), Prymnesiophyceae (two species), Cryptophyceae (five species), Prasinophyceae (two species), and Cyanophyceae (three species). Some of the cells were identified only to the genus level. Small flagellates and juvenile stages in the life cycle of dinoflagellates presented considerable difficulties to identification. In these cases, cells were measured during examination to calculate their volume and order them

according to size categories. We took into account flagellates with a cell diameter $>5\text{--}6 \mu\text{m}$.

Table 2 lists the algal species not mentioned in the available literature as components of the phytocenoses in the examined region [1, 2, 4, 6, 15, 16, 18, 20, 22, 23]. Some of the species from this list are widespread in Arctic seas and significantly contribute to the total abundance and biomass of phytoplankton in the Laptev Sea.

The species composition of plankton algae makes it possible to distinguish two distinctly different phytoplankton complexes, namely southern and northern. The species belonging to the classes Bacillariophyceae, Chlorophyceae, and Cyanophyceae were dominant in the southern complex, established under the influence of freshwater Lena River discharge (Fig. 4). Bacillariophyceae were prevalent at three of the four stations located in the region with the maximum influence of freshwater discharge (stations 5216–5219). Several *Aulacoseira* species (*A. granulata*, *A. distans*,

Table 2. List of phytoplankton species of Laptev Sea not mentioned in available literature [2–4, 6, 12, 14, 16, 17, 20] (abundance, cells/L)

Taxa	Ecological characterization	Biogeographic characterization	Maximum species (genus) abundance in our samples
Bacillariophyceae			
<i>Chaetoceros borealis</i>	M	B–A (C?)	110
<i>Chaetoceros gracilis</i>	M and E	C	7500
<i>Chaetoceros simplex</i>	N	B?	16800
<i>Chaetoceros subtilis</i>	Br	B	15450
<i>Chaetoceros teres</i>	M	B–A	400
<i>Diatoma vulgare</i>	S	B–A	200
<i>Hemiaulus hauckii</i>	M	B	200
<i>Eucampia zodiacus</i>	M	C	1100
<i>Fragilaria capucina</i>	S and E	C	72850
<i>Fragilaria crotonensis</i>	S and E	B	17100
<i>Fragilaria striatula</i>	N	B–A	80
<i>Fragilaria (Ulnaria) ulna</i>	S	C	200
<i>Fragilariopsis oceanica</i>	M	A	500
<i>Nitzschia longissima</i>	N, E	C	4520
<i>Rhizosolenia hebetata</i> f. <i>hebetata</i>	M	B–A	560
<i>Roperia tessellata</i>	M	C	430
<i>Skeletonema subsalsum</i>	Br	B?	8700
Dinophyceae			
<i>Actiniscus pentasterias</i>	M	C	40
<i>Alexandrium</i> sp.			40
<i>Amphidinium sphaenoides</i>	P	B–A	40
<i>Cochlodinium</i> sp.	N	B	50
<i>Dinophysis acuminata</i>	N and E	T–B–A	2690
<i>Gymnodinium simplex</i>	N	T–A–B	1600
<i>Gymnodinium vitiligo</i>	N	B	750
<i>Gymnodinium veneficum</i>	N	B	450
<i>Gymnodinium wulffii</i>	P	B	200
<i>Gyrodinium aureolum</i>	M	B	40
<i>Gyrodinium fusiforme</i>	P	T–B–A	120
<i>Gyrodinium lachryma</i>	P	B–A	50
<i>Gyrodinium pinque</i>	N	B	130
<i>Gyrodinium spirale</i>	N	K	20
<i>Heterocapsa triquetra</i>	P and E	B (C)	6500
<i>Katodinium glaucum</i>	N	B–T (C)	260
<i>Katodinium rotundatum</i>	N	B–T	1620
<i>Prorocentrum</i> sp.			2270
<i>Protoceratium reticulatum</i>	N	B	20
Chlorophyceae			
<i>Ankistrodesmus falcatus</i>	S	A–B	7350
<i>Ankistrodesmus fusiformis</i>	S	A–B	23900
<i>Chlorella</i> sp.	S		33100
<i>Coelastrum</i> sp.	S		200

Table 2. (Contd.)

Taxa	Ecological characterization	Biogeographic characterization	Maximum species (genus) abundance in our samples
<i>Coenochloris fottii</i>	S	A–B	800
<i>Dictyosphaerium ehrenbergianum</i>	S	A–B	1500
<i>Dictyosphaerium pulchellum</i>	S	A–B	5450
<i>Monoraphidium arcuatum</i>	S	A–B	620
<i>Monoraphidium contortum</i>	S	A–B	20300
<i>Monoraphidium griffithii</i>	S	A–B	5120
<i>Pediastrum duplex</i>	S	A–B	60
<i>Pediastrum biradiatum</i>	S	A–B	460
<i>Scenedesmus acuminatus</i>	S	A–B	1700
<i>Scenedesmus arcuatus</i>	S	A–B	7700
<i>Scenedesmus parvus</i>	S	A–B	2840
<i>Scenedesmus quadricauda</i>	S		10200
<i>Oocystis</i> sp.	S		70
Chrysophyceae			
<i>Calycomonas wulffii</i>	P	A–B?	12750
<i>Meringosphaera tenerrima</i>	N	A–B	2750
<i>Olisthodiscus luteus</i>	N and E	B	1000
Cryptophyceae			
<i>Hillea fusiformis</i>	N	B	5000
<i>Leucocryptos marina</i>	P	B–A	860
<i>Plagioselmis prolonga</i>	N	B	7730
<i>Rhodomonas</i> sp.			30
Prasinophyceae			
<i>Pyramimonas grossii</i>	P	C	41600
<i>Tetraselmis</i> sp.	N	B	950
Euglenophyceae			
<i>Eutreptiella braarudii</i>	N	B–A	550
<i>Eutreptiella</i> sp.			2550
Dictyochophyceae			
<i>Parapedinella reticulata</i>	N	B	80
Cyanophyta			
<i>Oscillatoria</i> sp.	P	T–B	230
Raphidophyceae			
<i>Olisthodiscus luteus</i>	Br	B?	1000

Numbers exceeding 10×10^3 cells/L are boldfaced; M, marine species; E, euryhaline; Br, brackish water; S, freshwater; N, neritic; P, panthalassic; A, Arctic; B, boreal; T, tropic; and C, cosmopolitan species; (?) species with indistinct biogeographic characterization.

and *A. italica*) were the most abundant. The maximum abundance of *Aulacoseira* species was observed in the surface layer at station 5216 (655×10^3 cells/L) and was associated with the minimum salinity (2.7 psu). The maximum abundances of *Fragilaria capucina* (73×10^3 cells/L), *Asterionella formosa* (50×10^3 cells/L), and *Diatoma elongatum* (63×10^3 cells/L) were recorded at the same site. As for the northern periphery of the max-

imally desalinated region (station 5219), green Chlorococcales were the most abundant there (Table 3, Fig. 4). The most abundant of them were *Ankistrodesmus fusiformis*, *A. falcatus*, *Monoraphidium contortum*, *Chlorella* sp., and several *Scenedesmus* species. There were extremely few blue-green algae.

The northern boundary of the biotope inhabited by the southern algal complex coincided with the frontal

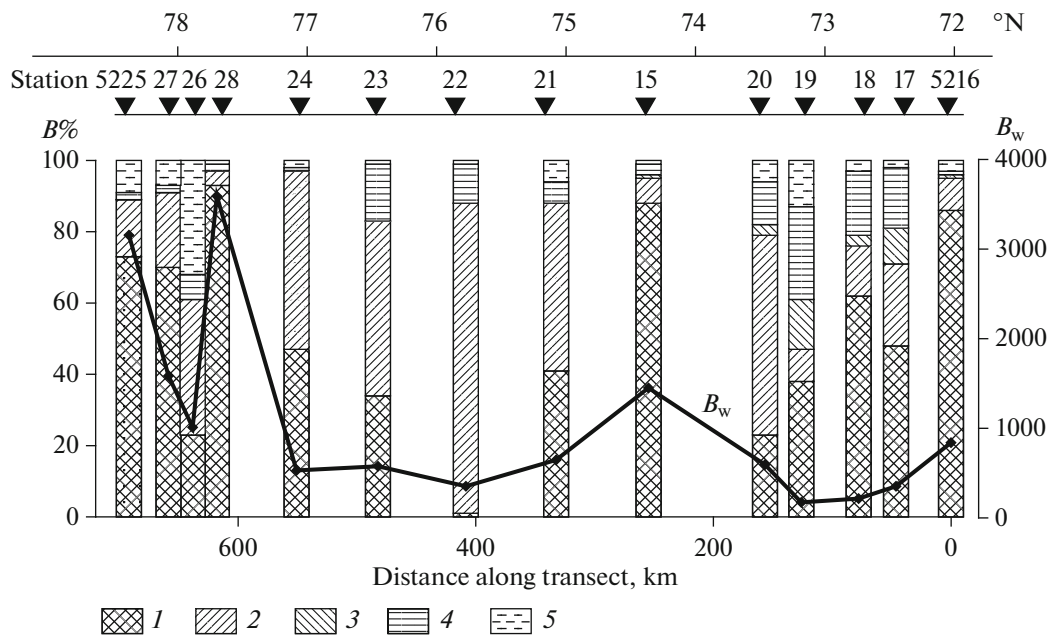


Fig. 4. Changes in total phytoplankton biomass (B_w , mg/m^2) and contributions (%) of different algal groups to total biomass along transect at $130^\circ30' \text{ E}$: (1) diatoms, (2) dinoflagellates, (3) green algae, (4) flagellates, and (5) others.

boundary in the periphery of the maximally desalinated shelf coastal zone, where salinity increased from 8 to 18 psu in the upper mixed layer, and was located between stations 5219 and 5220 ($73^\circ30' - 74^\circ00' \text{ N}$) (Figs. 1, 2a). Only a few freshwater species were observed beyond this region, and their numbers did not exceed 1000–2000 cells/L. The group that displayed the highest salinity tolerance was green algae of the genera *Scenedesmus* and *Monoraphidium* (in particular, *M. arcuatum* and *M. griffithii*). Note that the spatial changes in the ratio of freshwater and marine species in the most desalinated southern shelf region (stations 5216–5219) were determined by the local impact of freshwater discharge from the Bykov and Trofimov Channels (Table 4, Fig. 5).

Dead cell counts in the populations of individual species belonging to the genus *Aulacoseira*, the most abundant among the freshwater diatoms, showed an increase in the relative abundance of dead cells with distance from the zone influenced by freshwater discharge and with sinking to layers under the pycnocline (Table 5). The abundance of *Aulacoseira* in the sample from a depth of 10 m (bottom layer) taken at station 5217 was six times higher compared with the surface layer and over one order of magnitude higher compared with the subsurface layer; at that dead cells accounted for ~60% of the total abundance observed for this genus.

The northern phytoplankton complex, observed north of $77^\circ30' \text{ N}$ at slope and deepwater stations 5225–5228, consisted of marine species widespread in Arctic seas. The abundance and biomass of the algae making up this complex during our study were mainly deter-

mined by centric diatoms and, to a lesser degree, by dinoflagellates. *Chaetoceros* algae were the most abundant among diatoms, in particular, the widespread Arctic–boreal species *C. debilis* and *C. decipiens*, neritic species *C. compressus*, and Arctic species *C. furcellatus*. The listed species were represented not only by vegetative cells, but also by spores (Table 6). *C. furcellatus* was observed almost completely as spores; presumably, it had completed its vegetation several weeks before our observations. Along with *Chaetoceros*, another Arctic–boreal species, *Rhizosolenia hebetata*, mainly *R. hebetata* f. *semispina*, was a significant contributor to the biomass of the northern phytoplankton complex. The dinoflagellate species *Heterocapsa triquetra*, *Ceratium arcticum*, *Protoperidinium pellucidum*, *P. brevipes*, and *Gymnodinium* sp. were a considerable component of the northern complex as well as the juvenile stages of dinoflagellates. The northern complex also contained *Dictyocha speculum*, a member of the class Dictyochophyceae.

Part of the species constituting the northern phytoplankton complex spread far southward to the area of the outer shelf and were observed at a salinity of 22 to 18 psu in the upper mixed layer. The dinoflagellates *Dinophysis acuminata*, *Protoperidinium bipes*, *P. pellucidum*, *Katodinium glaucum*, *K. rotundatum*, *Gymnodinium vitiligo*, *Gyrodinium fusiforme*, *G. pinque*, and *Heterocapsa triquetra* and the diatoms *Chaetoceros wighamii*, *C. subtilis*, *C. gracilis*, and *Thalassionema nitzschioides* were among these species. Among the other algal species and groups, weakly desalinated area of the outer shelf was home to *Dinobryon balticum*,

Table 3. Phytoplankton total abundance ($N \times 10^6$ cells/m²) and biomass (B , mg/m²), abundance and biomass of individual algal groups, and their contribution (%) to total abundance and biomass

Station no.	Layer, m	Total		Diatoms		Dinoflagellates		Green		Flagellates	
		<i>N</i>	<i>B</i>	<i>N</i>	<i>B</i>	<i>N</i>	<i>B</i>	<i>N</i>	<i>B</i>	<i>N</i>	<i>B</i>
5216	0–6	2025.0	840.0	1940.0	722.5	16.2	71.8	53.1	7.5	5.3	10.1
	%			<i>94.1</i>	<i>86.0</i>	<i>0.8</i>	<i>8.5</i>	<i>2.6</i>	<i>0.9</i>	<i>0.3</i>	<i>1.2</i>
5217	0–10	655.8	353.7	463.1	169.3	11.6	80.3	70.3	36.4	86.0	61.2
	%			<i>70.6</i>	<i>47.9</i>	<i>1.8</i>	<i>22.7</i>	<i>10.7</i>	<i>10.3</i>	<i>13.1</i>	<i>17.3</i>
5218	0–10	426.0	216.0	228.4	133.0	39.0	31.2	64.3	6.2	82.0	39.6
	%			<i>53.6</i>	<i>61.6</i>	<i>9.2</i>	<i>14.4</i>	<i>15.1</i>	<i>2.9</i>	<i>19.2</i>	<i>18.3</i>
5219	0–10	398.0	174.0	100.0	65.1	14.8	15.3	164.6	25.0	91.8	45.2
	%			<i>25.1</i>	<i>37.5</i>	<i>3.7</i>	<i>8.8</i>	<i>41.4</i>	<i>14.4</i>	<i>23.1</i>	<i>26.0</i>
5220	0–14	1216.7	593.5	240.2	138.1	233.4	330.7	146.0	19.5	259.5	71.2
	%			<i>19.8</i>	<i>23.3</i>	<i>19.2</i>	<i>55.7</i>	<i>12.0</i>	<i>3.3</i>	<i>21.3</i>	<i>12.0</i>
5215	0–16	2025.3	1450.4	1331.0	1271.0	80.3	99.8	6.6	2.4	411.6	59.6
	%			<i>66.2</i>	<i>87.6</i>	<i>4.0</i>	<i>6.9</i>	<i>0.3</i>	<i>0.2</i>	<i>20.5</i>	<i>4.1</i>
5221	0–15	578.0	646.0	98.8	262.5	117.8	303.0	–	–	190.4	40.7
	%			<i>17.1</i>	<i>40.6</i>	<i>20.4</i>	<i>46.9</i>			<i>32.9</i>	<i>6.3</i>
5222	0–15	406.8	353.0	1.2	1.5	152.8	306.0	+	+	237.6	42.2
	%			<i>0.3</i>	<i>0.4</i>	<i>37.6</i>	<i>86.7</i>			<i>58.4</i>	<i>12.0</i>
5223	0–15	366.3	576.0	10.4	192.8	89.6	287.6	+	+	257.6	89.4
	%			<i>2.8</i>	<i>33.5</i>	<i>24.5</i>	<i>49.9</i>			<i>70.3</i>	<i>15.5</i>
5224	0–20	117.0	530.1	10.1	247.2	90.9	206.4	–	–	8.4	2.8
	%			<i>8.6</i>	<i>46.6</i>	<i>77.7</i>	<i>50.3</i>			<i>7.1</i>	<i>0.5</i>
5228	0–22	548.9	3592.2	424.7	3332.1	40.4	157.1	–	–	16.1	6.0
	%			<i>77.4</i>	<i>92.8</i>	<i>7.4</i>	<i>4.4</i>			<i>2.9</i>	<i>0.2</i>
5226	0–27	434.7	1010.4	61.6	235.3	165.1	386.8	–	–	66.5	67.0
	%			<i>14.2</i>	<i>23.3</i>	<i>38.0</i>	<i>38.3</i>			<i>15.3</i>	<i>6.6</i>
5227	0–27	707.1	1585.5	333.7	1116.4	165.3	335.6	–	–	146.9	35.1
	%			<i>47.2</i>	<i>70.4</i>	<i>23.4</i>	<i>21.2</i>			<i>20.8</i>	<i>2.2</i>
5225	0–25	1114.0	3155.0	668.3	2297.0	187.5	508.5	–	–	155.1	44.3
	%			<i>60.0</i>	<i>72.8</i>	<i>16.8</i>	<i>16.1</i>			<i>13.9</i>	<i>1.4</i>
5230	0–20	325.3	1929.0	125.7	1539.0	135.0	317.6	–	–	9.8	18.8
	%			<i>38.6</i>	<i>79.8</i>	<i>41.5</i>	<i>16.5</i>			<i>3.0</i>	<i>1.0</i>

Contribution of group to total abundance and biomass (%) is italicized.

Calycomonas wulfii, *Pyramimonas* sp., and Cryptophyceae.

A mosaic spatial structure of the phytocenosis was observed in the region of the outer shelf (stations 5220–5224) separating the coastal (most desalinated) and the deepwater sea regions and inhabited by the southern and northern phytoplankton complexes, respectively

(Table 3, Fig. 4). In particular, Prasinophyceae (24.6%), flagellates (21.3%), Bacillariopyceae (19.8%), and Dinophyceae (19.2%) were observed at station 5220 with almost equal abundances and flagellates (32.9%), Dinophyceae (20.4%), Cryptophyceae (22.0%), and Bacillariopyceae (17.1%), at station 5221. Stations 5222 and 5223 characteristically showed a very

Table 4. Abundance ($N \times 10^6$ cells/m²), wet biomass of phytoplankton (B_{wet} , mg/m²), biomass in carbon units (B_c , mg/m²), contribution of marine species (%_{ms}), chlorophyll *a* concentration (Chl *a*, mg/m²), and mean algae cell weight (W , pg) in photosynthetic layer along transect

Station, layer	N	B_{wet}	B_c	Chl <i>a</i>	W
5216, 0–6 m	2025.0	840.0	122.0	7.1	415
% _{ms}	3.2	26.6	15.1		
5217, 0–10 m	655.8	353.7	49.1	7.7	540
% _{ms}	4.8	30.9	26.5		
5218, 0–10	426.0	216.0	29.3	4.0	507
% _{ms}	28.2	38.2	35.5		
5219, 0–10	397.9	174.1	23.5	3.4	435
% _{ms}	14.4	37.6	32.6		
5220, 0–14	1216.7	593.5	67.9	8.7	490
% _{ms}	67.6	85.7	86.1		
5215, 0–16	2010.6	1450.4	164.9	8.3	720
% _{ms}	98.5	97.9	97.2		
5221, 0–15	578.0	646.0	64.2	6.3	1120
% _{ms}	100	100	100		
5222, 0–15	406.8	353.0	37.7	6.2	870
% _{ms}	99.95	99.9	99.9		
5223, 0–15	366.3	576.0	52.6	4.3	1500
% _{ms}	99.5	99.7	99.5		
5224, 0–2	117.0	530.1	37.1	1.1	4500
% _{ms}	100	100	100		
5228, 0–22	548.9	3592.2	166.2	7.6	6540
% _{ms}	100	100	100		
5226, 0–2	434.7	1010.4	110.3	8.4	2325
% _{ms}	100	100	100		
5227, 0–27	707.1	1585.5	106.1	7.5	2240
% _{ms}	100	100	100		
5225, 0–25	1114.0	3155.0	278.5	9.6	2830
% _{ms}	100	100	100		
5230, 0–20	325.3	1929.0	99.7	7.5	5900
% _{ms}	100	100	100		

low abundance of diatoms (0.3 and 2.8% of the total cell numbers, respectively), maximum abundance of flagellates (58.4 and 70.3%, respectively), and dominance of Dinophyceae in the biomass. As for station 5224, juve-

nile stages of Dinophyceae were dominant in abundance, accounting for 48% of the total cell counts.

Phytoplankton Abundance and Biomass

The phytoplankton abundance and wet biomass in the photosynthetic layer of the studied region varied in a very wide range, from 117×10^6 cell/m² (6×10^3 cells/L) to 2025×10^6 cell/m² (340×10^3 cells/L) and from 174 (17.4 mg/m³) to 3592 mg/m² (163.3 mg/m³), respectively (Figs. 5, 6).

The highest phytoplankton abundance was recorded at stations 5216 and 5215-2 (Table 4, Fig. 5) as well as a high algal biomass, amounting to 178.0 mg/m³ at station 5216 and 97 mg/m³ at station 5215-2. Diatoms were dominant at both stations, accounting for 96.0 and 68% of the total phytoplankton abundance and 97.0 and 89.0% of the total biomass, respectively (Fig. 4). These stations fundamentally differ in the environmental conditions and composition of the phytocenosis. Station 5216 was located in the most desalinated coastal region (Fig. 2a), where the freshwater diatom complex was dominating and *Aulacoseira* species accounted for 78.0% of the total diatom cell numbers. As for station 5215-2, localized at the southern boundary of the desalinated outer shelf region, where the pycnocline rises to the surface and the euphotic zone is enriched in nutrients, the marine diatom complex was dominant and several *Chaetoceros* species accounted for 92.2% of the total diatom cell numbers. The vertical distribution of algae also considerably differed. The maximum cell numbers at station 5216 were associated with the surface layer residing above the density jump, similar to the overall coastal shelf region most desalinated by the Lena River discharge (Fig. 7). The majority of phytoplankton at station 5215-2 were concentrated in the lower part of the photosynthetic layer at a depth of 10 m (Fig. 7).

The highest values of wet phytoplankton biomass, carbon biomass, and chlorophyll *a* concentration for the entire study area amounted to 174.8, 25.0, and 1.2 mg/m³, respectively, and were observed in the southernmost maximally desalinated part of the transect (station 5216) in the photosynthetic layer (Table 4). Note that 75% of the total phytoplankton biomass were concentrated in the upper 2-m layer, where the maximum chlorophyll *a* concentrations were also observed (Fig. 7). At the same station, the populations of dominant *Aulacoseira* species displayed the lowest rate of dead cells (Table 5). Station 5216 was directly influenced by the freshwater discharge from the Bykov Channel. The rates of dead cells in *Aulacoseira* populations at the stations in the rest of coastal maximally desalinated shelf region were considerably higher, mainly (Table 5), suggesting degradation of the freshwater phytocenosis with the distance from the mouth of the channel.

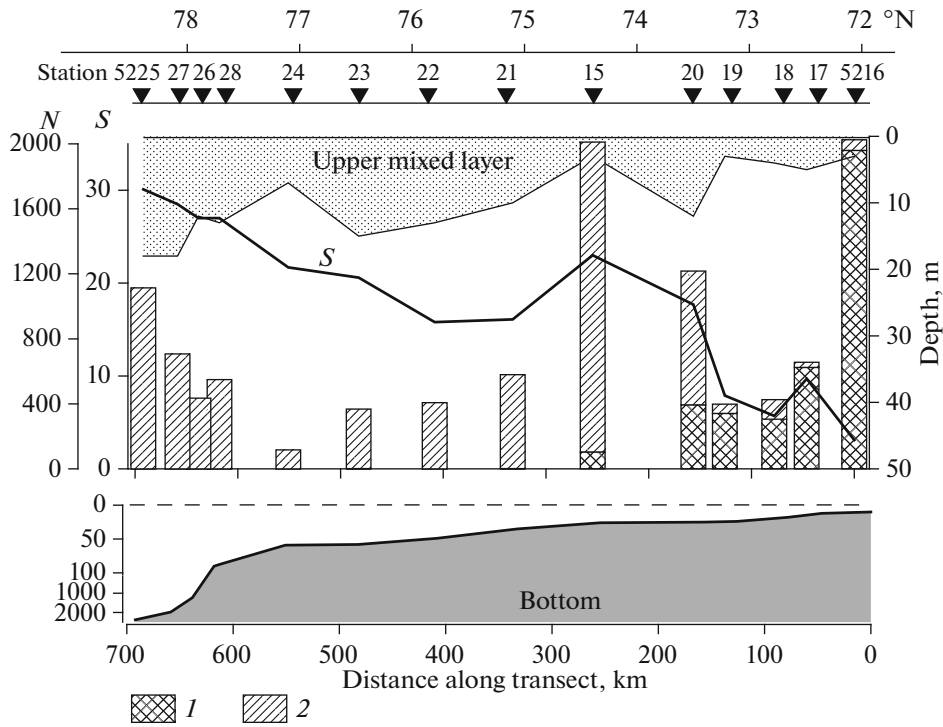


Fig. 5. Distribution of salinity (S , psu) and contributions of freshwater and marine algal species to total phytoplankton abundance ($N \times 10^3$ cells/m³) along transect at 130°30' E: (1) freshwater and (2) marine species.

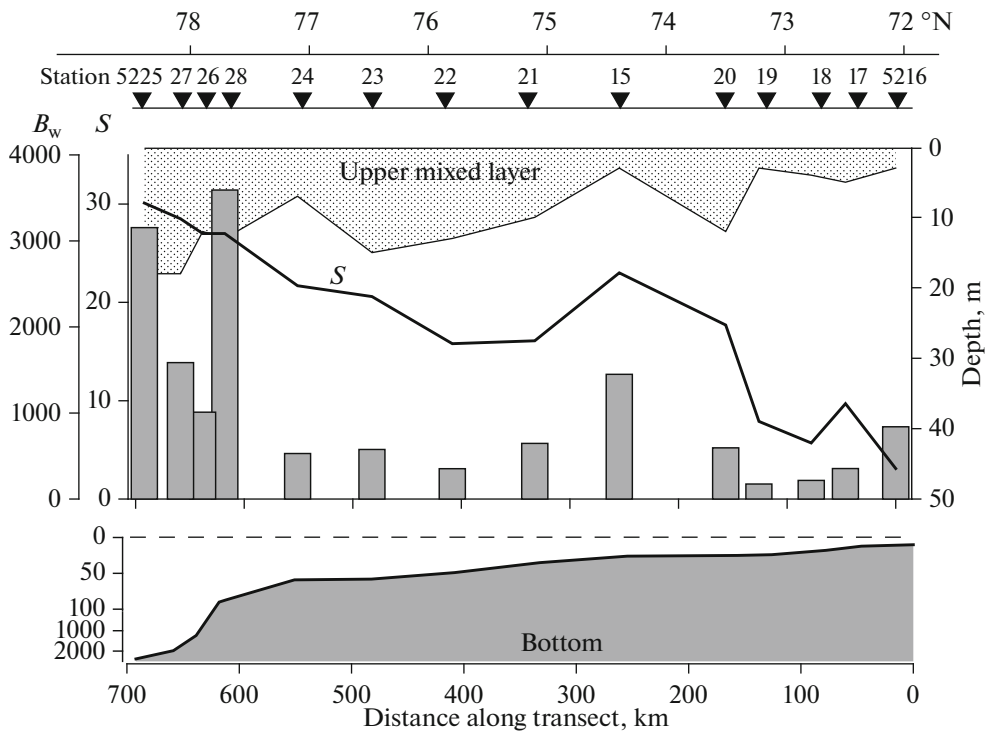


Fig. 6. Distributions of salinity (S , psu) and total phytoplankton biomass (B_w , mg/m²) along transect at 130°30' E.

Table 5. Structure of *Aulacoseira* populations in the most desalinated inner shelf area: total abundance of *Aulacoseira* (N_{total}), counts of live (N_{live}) and dead (N_{dead}) cells ($N \times 10^3$ cells/L), and percentage of dead cells ($\%_{\text{dead}}$) in total *Aulacoseira* numbers

Station no.	Horizon, m	N_{total}	N_{live}	N_{dead}	$\%_{\text{dead}}$
5216	0	705.8	655.6	50.2	7.1
	3	220.1	199.7	20.4	9.3
	6	13.4	11.9	1.5	11.2
5217	0	25.9	19.2	6.7	25.9
	4	4.0	2.7	1.3	32.5
	10*	160.1	68.6	91.5	57.2
5218	0	38.3	29.8	8.5	22.2
	4	17.7	4.7	13.0	73.4
	9	1.3	0.6	0.7	53.8
	17	1.7	—	1.7	100.0
5219	0	17.4	11.0	6.4	36.8
	4	9.9	6.4	3.5	35.4
	8	22.6	2.9	19.7	87.2
	15	3.9	—	3.9	100.0
5220	0	1.3	0.5	0.8	61.5
	5	0.7	0.2	0.5	71.4
	10	19.1	3.2	15.9	83.2

* Samples from bottom layer contain ~90% of live cells with altered chloroplast.

Characteristic of stations 5220 and 5225 was a comparatively high algal abundance. Station 5220 was near the frontal boundary in the northern periphery of the coastal region desalinated by the riverine discharge and displayed a considerable increase in salinity in the upper mixed layer (from 8 to 18 psu), decrease in the concentration of suspended matter to 1.5 mg/L, and manifold increase in transparency; however, the concentration of nitrates in the photosynthetic layer remained at the level of 3.0–3.5 μM , which is characteristic of the coastal shelf zone. The freshwater phytoplankton abundance, characteristic to the most desalinated shelf region, drastically decreased at station 2220, whereas the abundance of marine species increased. The maximum algal abundance and biomass of 107×10^3 cells/L and 62 mg/m³, respectively, were recorded in the subsurface layer at a depth of 5 m (Fig. 7).

Several *Chaetoceros* species of the northern complex accounted for over 50% of the high phytoplankton abundance at station 2552; at that half the cells were represented by spores (Table 6). The vertical distribution of phytoplankton abundance in the upper 20 m was uniform, which was determined by high transparency and deep position of the gradient layer (Fig. 7).

The northern phytoplankton complex at deepwater stations 5225–5227 and slope station 5228 had the

highest biomass in the study area (Table 4, Fig. 6). The maximum biomass at stations 5225 and 5228 resulted from a high abundance of large-celled *Chaetoceros* species (mean cell volume, $3 \times 10^3 \mu\text{m}^3$), *Rhizosolenia hebetata* f. *semispina* (mean cell volume, 13×10^3 to $27 \times 10^3 \mu\text{m}^3$), and auxospores of the latter (cell volume, 30×10^3 to $70 \times 10^3 \mu\text{m}^3$). At stations 5225 and 5228, *R. hebetata* accounted for 64.1 and 43.0% of the total phytoplankton biomass, respectively. Spores considerably contributed to the abundance and biomass of *Chaetoceros* populations at stations 5225–5228; their relative content increased with depth and reached 80–100% below 20 m (Table 6).

DISCUSSION

Our studies and the data of earlier works reveal distinct latitudinal zoning in the structure of phytoplankton communities of the Laptev Sea (Fig. 8).

The southern shelf region, maximally desalinated by the Lena River discharge, housed a phytoplankton community with the prevalence of freshwater algal species (accounting for 71.8–96.8% of the total phytoplankton abundance; Table 4, Fig. 8). The southern complex of phytoplankton species displayed a high total biomass (175–840 mg/m²; Fig. 6), dominance of freshwater diatoms, significant contribution of green algae to both abundance and biomass (Table 3, Fig. 4), and moderate average algae cell volume (~500 μm^3). In our study, considerably desalinated surface water and latitudinal distribution of the southern complex of phytoplankton species were traceable to 73° N. However, it is evident that the northern boundary for the distribution of the southern complex with its dominance of freshwater forms is not distinctly associated with particular coordinates and shifts depending on the Lena River discharge intensity and the distribution of surface salinity over the Laptev Sea shelf. It is possible to rather distinctly associate this boundary with a certain salinity level in the upper mixed layer, which is confirmed by the data for the region with significant influence of the Lena River discharge as well as for the Ob and Yenisei River estuaries [10, 13, 16, 22]. In our study, the boundary was distinct and confined to between the 8 and 18 psu isohalines.

The previous studies in the Lena River delta and Laptev Sea shelf also distinguished a community associated with the plume desalinated by the riverine discharge and differing in both its composition and quantitative characteristics (Table 7) and allowed for drawing of the northern boundary of the inner shelf desalinated zone with its prevalent freshwater phytoplankton complex [16, 22]. Sorokin and Sorokin [22] draw this boundary along the 15 psu isohaline, while other researchers associate this boundary with the 13 psu isohaline. It was difficult to determine this boundary with rather large distance between stations and under high latitudinal gradient conditions over the

Table 6. Structure of *Chaetoceros* populations: abundance ($N \times 10^3$ cells/L) and share of spores (%) in total *Chaetoceros* numbers

Station no.	Horizon, m	N , total	N , vegetative cells	N , spores	Spores, %
5228	0	12.6	12.6	0	0
	10	23.1	22.0	1.1	4.8
	20	3.7	1.8	1.9	51.4
	35	0.2	0	0.2	100.0
5226	0	0.2	0.2	0	0
	12	3.0	0.8	2.2	73.3
	20	0.4	0.2	0.2	50.0
	35	8.2	0	8.2	100.0
5227	0	4.1	2.2	1.9	46.3
	12	19.4	4.4	15.0	77.3
	18	2.6	1.9	0.7	27.0
	32	22.8	2.5	20.3	89.0
5225	0	19.2	13.0	6.2	32.3
	10	31.0	23.4	7.6	24.5
	15	24.7	4.9	19.8	80.2
	24	10.2	1.9	8.3	81.4

Table 7. Quantitative phytoplankton characteristics: abundance ($N \times 10^3$ cells/L), wet biomass (B_{wet} , mg/m³), carbon biomass (B_c , mg/m³), and chlorophyll *a* concentration (Chl *a*, mg/m³) in surface layer in studied region according to data of different researchers

Region	Parameter	Our data (September 8–9)	Sorokin and Sorokin [22], average for examined region (September 4–9)	Heiskanen and Keck [16], average for examined region (September 3–8)
Inner shelf region most desalinated by Lena River discharge (>8 psu)	N	60–850	140.0	520
	B_{wet}	50–345		
	B_c	7–52		
	Chl <i>a</i>	0.6–1.2		
Surface “lens” in shelf desalinated by riverine discharge (18–22 psu)	N	40–106	70.0	75.0
	B_{wet}	33–62		
	B_c	3.1–7.3		
	Chl <i>a</i>	0.4–0.9		

shelf; correspondingly, these differences should not be regarded as basic. However, the authors distinctly distinguished the southern phytoplankton complex with its prevalence of freshwater diatoms, the distribution of which was associated with the inner shelf of the Laptev Sea desalinated by the Lena River discharge [16, 22, 23].

According to our data, the continental slope and deepwater regions north of 77°30' N were populated by the northern phytoplankton complex distinctly different in its species composition and biomass (Table 4). This complex comprised marine species widespread in the Arctic seas. In addition to large-sized diatom species

Chaetoceros and *Rhizosolenia*, dinoflagellates played a significant role in the northern phytoplankton complex. The average algae cell size was 8 fold larger as compared with the southern complex and amounted to ~4000 μm^3 ; the phytoplankton cell numbers were 430–1100 $\times 10^6$ cells/m² and biomass, 1010–3600 mg/m². The contributions of diatoms to the abundance and biomass were 14–80 and 23–93%, respectively, and of dinoflagellates, 7–42 and 4–38%. The major factor that limited a latitudinal expansion of the northern algal species complex (as well as of the southern complex) was salinity. The southern boundary of the area occupied by the northern phytoplankton complex was

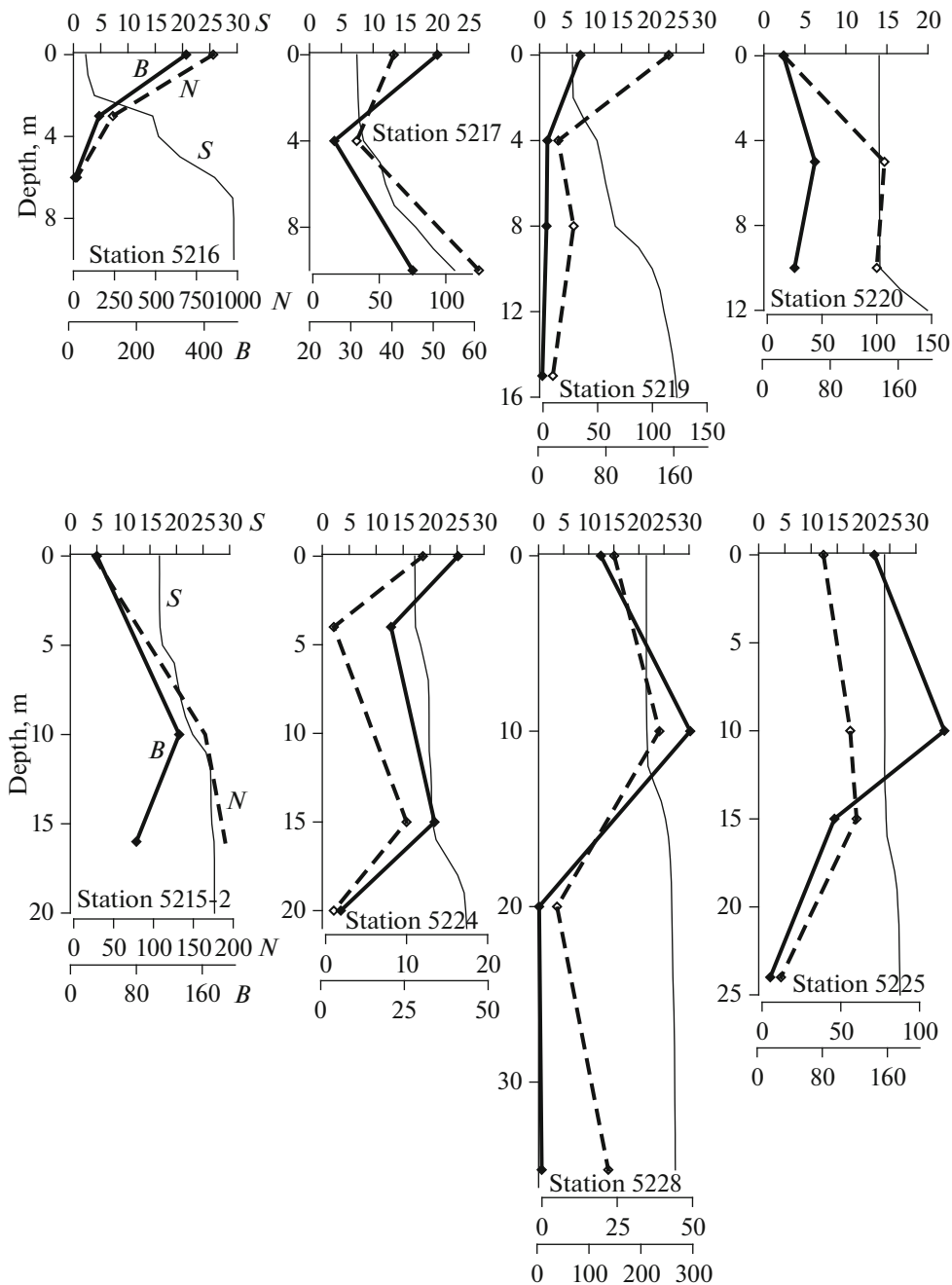


Fig. 7. Vertical distributions of salinity (S , psu), phytoplankton abundance ($N \times 10^3$ cells/ m^3), and biomass (B , mg/m^3) at stations of transect along $130^\circ 30' E$.

associated with the boundary of the desalinating impact caused by the Lena River discharge on the properties of the upper mixed layer, where salinity increased northward from 22 to 27 psu (Figs. 2, 8).

All earlier studies of the Laptev Sea phytoplankton considered neither the deepwater part of the basin nor the continental slope. Only Fahl et al. [15] mentioned the northern phytoplankton complex with a considerable contribution of dinoflagellates and its southern

boundary associated with a salinity of 24–25 psu based on the analysis of algal remains in surface sediments.

Thus, diatoms were dominant in the eastern part of the Laptev Sea in the southern shelf region, maximally desalinated by riverine discharge, and in the northern deepwater region with the maximum salinity of the upper mixed layer in the first half of September and the early fall period of succession (Figs. 4, 8). Salinity was the major factor limiting the distribution of dia-

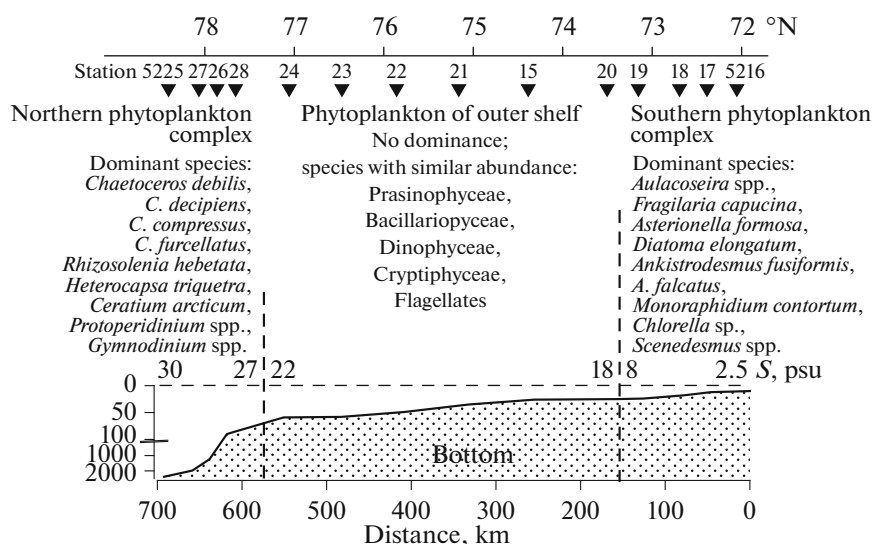


Fig. 8. Latitudinal zoning in structure of phytoplankton communities of Laptev Sea.

toms belonging to both southern and northern algal species complex.

The region of the outer shelf between 73°20' and 77°30' N during our studies was moderately desalinated by the Lena River discharge. The salinity in the upper mixed layer smoothly increased from 18 to 22 psu from south to north. Characteristically, this region had a mosaic spatial structure of the phytocenosis with a drastic change in the shares of different algal groups of the community from station to station. The share of freshwater species in the total phytoplankton abundance and biomass in this region was below several percent. Typical algal cell numbers were $117\text{--}1200 \times 10^6$ cells/m², and the biomass was 350–590 mg/m².

The latitudinal zoning in the structure of phytoplankton communities of the Laptev Sea is also evident according to diatom remains in current surface sediments [15]. Fahl et al. [15] distinguished several communities within the sea area confined by the 40-m isobathic line. The community with the prevalence of freshwater species occupied the coastal desalinated zone to 74° N, followed northward (to 76° N) by the community of ice algae with local areas of high abundance of *Thalassiosira nordenskioldii* and *Chaetoceros* spores. *Chaetoceros* represented by spores were dominant in the region north of the New Siberian Islands (~76° N) and east of 134° E.

The specific local features in hydrophysical structure and phytoplankton quantitative characteristics at station 5215-2 deserve special consideration. The phytoplankton abundance there reached the level close to the maximum for the overall examined area (2010×10^6 cells/m²), and biomass was the highest for the entire shelf region, 1450 mg/m² (Table 4, Figs. 4, 6). Marine diatoms distinctly dominated in the phytocenosis. Several *Chaetoceros* species contributed significantly

to the community, accounting for 62% of the total phytoplankton abundance and 74% of the total biomass. The share of freshwater component in abundance and biomass did not exceed 3%.

Station 5215-2 was at the edge of the surface water “lens” desalinated by riverine discharge; the “lens” resided in the outer shelf between stations 5215-2 and 5224 (Fig. 2). The depth of the upper mixed layer at the periphery of the “lens” drastically decreased to 4 m. In addition, relatively high concentrations of nitrates (5.2 μM), the most important nutrient for phytoplankton growth over the Arctic shelf, associated with the pycnocline and underlying horizons (depth, 5–15 m), were recorded in the photosynthetic layer (thickness, 12 m). The phytoplankton abundance at these depths reached $165\text{--}190 \times 10^3$ cells/L, and the biomass was 80–132 mg/m³, which determined high values of these parameters for this station as a whole.

The local processes and relative phytoplankton abundance at station 5215-2 explain the extremely low algal abundance and the biomass, which is characteristic not only of the Laptev Sea shelf, but also of the other epicontinental Siberian Arctic seas in the summer and fall seasons. The reason is the low concentrations of nutrients, primarily nitrates in the photosynthetic layer, which limits phytoplankton growth. This is related to the rigid density (salinity) vertical stratification of the water column in the shelf, which blocks vertical mixing and is associated with a large-scale desalinating effect of riverine discharge. The phenomenon of rising of the seasonal pycnocline to the surface at the periphery of regions desalinated by riverine discharge [3] and the related increase in available nutrients in the photosynthetic layer, entailing a considerable increase in phytoplankton abundance and biomass, was also described for the Kara Sea [11, 12].

ACKNOWLEDGMENTS

The authors thank the anonymous reviewer for careful analysis of the manuscript and helpful criticism.

The work was supported by the Russian Science Foundation under project nos. 14-50-00095 (field studies) and 14-17-00681 (sampling and processing of hydrophysical and hydrochemical data) and the Russian Foundation for Basic Research under project no. 16-05-00055 (processing of phytoplankton samples and primary data).

REFERENCES

1. A. Yu. Gukov, *Hydrobiology of the Estuary Area of the Lena River* (Nauchnyi Mir, Moscow, 2001) [in Russian].
2. E. I. Druzhkova and P. R. Makarevich, "Analysis of phytoplankton of the Laptev Sea: history and present," *Tr. Karel. Nauch. Tsentra, Ross. Akad. Nauk*, No. 1 (14), 71–79 (2013).
3. A. G. Zatsepin, P. O. Zavialov, V. V. Kremenetskiy, S. G. Poyarkov, and D. M. Soloviev, "The upper desalinated layer in the Kara Sea," *Oceanology (Engl. Transl.)* **50**, 657–667 (2010).
4. V. V. Zernova, E.-M. Nöthig, and V. P. Shevchenko, "Vertical microalga flux in the northern Laptev Sea (from the data collected by the yearlong sediment trap)," *Oceanology (Engl. Transl.)* **40**, 801–808 (2000).
5. A. P. Lisitzyn and M. D. Kravchishina, "Geological and geochemical analysis of suspended matter," in *The White Sea System*, Vol. 3: *Suspended Sedimentary Matter of Hydrosphere, Microbial Processes, and Pollution* (Nauchnyi Mir, Moscow, 2013), pp. 43–52.
6. A. M. Nikanorov, V. V. Ivanov, and V. A. Bryzgalov, *Rivers of Russian Arctic in Affected by Modern Anthropogenic Impact* (NOK, Rostov-on-Don, 2007) [in Russian].
7. *The System of the Laptev Sea and Adjacent Arctic Seas* (Moscow State Univ., Moscow, 2009) [in Russian].
8. S. F. Timofeev, "Pelagic ecosystem of the Laptev Sea," in *Biological Coastal Resources of Russian Arctic* (All-Russian Scientific Research Institute of Marine Fisheries and Oceanography, Moscow, 2000), pp. 137–139.
9. I. N. Sukhanova, "Concentrating of phytoplankton in a sample," in *Modern Methods of Quantitative Assessment of Distribution of Marine Plankton* (Nauka, Moscow, 1983), pp. 97–105.
10. I. N. Sukhanova, M. V. Flint, S. A. Mosharov, and V. M. Sergeeva, "Structure of the phytoplankton communities and primary production in the Ob River estuary and over the adjacent Kara Sea shelf," *Oceanology (Engl. Transl.)* **50**, 743–758 (2010).
11. I. N. Sukhanova, M. V. Flint, and V. M. Sergeeva, "Phytoplankton of the surface desalted lens of the Kara Sea," *Oceanology (Engl. Transl.)* **52**, 635–645 (2012).
12. I. N. Sukhanova, M. V. Flint, E. I. Druzhkova, A. F. Sazhin, and V. M. Sergeeva, "Phytoplankton in the northwestern Kara Sea," *Oceanology (Engl. Transl.)* **55**, 547–560 (2015).
13. I. N. Sukhanova, M. V. Flint, V. M. Sergeeva, E. I. Druzhkova, and A. A. Nedospasov, "Structure of phytoplankton communities in the Yenisei estuary and over the adjacent Kara Sea shelf," *Oceanology (Engl. Transl.)* **55**, 844–857 (2015).
14. H. A. Bauch, H. Kassens, H. Erlenkeuser, et al., "Depositional environment of the Laptev Sea (Arctic Siberia) during the Holocene," *Boreas* **28**, 194–204 (1995).
15. K. Fahl, H. Cremer, H. Erlenkeuser, et al., "Sources and pathways of organic carbon in the modern Laptev Sea (Arctic Ocean): implications from biological, geochemical and geological data," *Polarforschung* **69**, 193–205 (1999).
16. A. Heiskanen and A. Keck, "Distribution and sinking rates of phytoplankton, detritus and particulate biogenic silica in the Laptev Sea and Lena River (Arctic Siberia)," *Mar. Chem.* **53**, 229–245 (1996).
17. O. Holm-Hansen and B. Riemann, "Chlorophyll *a* determination: improvements in methodology," *Oikos* **30**, 438–447 (1978).
18. A. C. Kraberg, E. Druzhkova, B. Heim, et al., "Phytoplankton community structure in the Lena delta (Siberia, Russia) in relation to hydrography," *Biogeosciences* **10**, 7263–7277 (2013).
19. S. Menden-Deuer and E. J. Lessard, "Carbon to volume relationships for dinoflagellates, diatoms and other protist plankton," *Limnol. Oceanogr.* **45** (3), 569–579 (2000).
20. Yu. B. Okolodkov, "A checklist of dinoflagellates recorded from Russian Arctic seas," *Sarsia* **83**, 267–292 (1998).
21. L. F. Small, C. D. McIntire, K. B. Macdonald, et al., "Primary production, plant and detrital biomass, and particle transport in the Columbia River estuary," *Prog. Oceanogr.* **25**, 175–210 (1990).
22. Yu. I. Sorokin and P. Yu. Sorokin, "Plankton and primary production in the Lena River estuary and in the south-eastern Laptev Sea," *Estuarine, Coastal Shelf Sci.* **43**, 399–418 (1996).
23. K. Tuschling, "Phytoplankton ecology in the arctic Laptev Sea—a comparison of three seasons," *Ber. Polarforsch.* **347**, (2000).
24. R. R. Strathmann, "Estimating the organic carbon content of phytoplankton from cell volume, cell area or plasma volume," *Limnol. Oceanogr.* **12** (3), 411–418 (1967).

Translated by G. Chirikova